

Effect of confinement on charge-stabilized colloidal suspensions between two charged plates

J. Chakrabarti

Laboratory of Separation Processes and Transport Phenomena, P.O. Box 513, 5600 MB Eindhoven, The Netherlands

H. Löwen*

Institute für Theoretische Physik II, Heinrich-Heine-Universität, Universitätsstrasse 1, D-40225 Düsseldorf, Germany

(Received 19 May 1998)

We study the effect of confinement on the phase behavior of a charge-stabilized colloidal suspension between two parallel charged plates. The electrostatic interaction of the counterions with the plates induces density inhomogeneity of the counterions. Our Monte Carlo simulations show that the external potential acting on the colloidal particles due to this inhomogeneity inhibits the *precrystallization* tendency, a prediction that can be verified in experiments. Our mean-field theory qualitatively accounts for the tendency to inhibit the precrystallization. [S1063-651X(98)11609-4]

PACS number(s): 82.70.Dd

INTRODUCTION

Monodisperse charge-stabilized colloidal suspensions are ideal model condensed matter systems to study various equilibrium and nonequilibrium phenomena found in atomic systems. This is because of the unique feature of colloidal suspensions, namely, very large length scales, for instance, large particle size and interparticle separation (approximately equal to the optical wavelength) and large time scale, i.e., very slow diffusion. Because of large interparticle separations, typical particle densities of the colloidal suspensions are about 10^{10} times less than in an atomic system and hence their shear moduli are low. This makes colloidal suspensions vulnerable to perturbations easily conceivable in laboratory conditions [1].

The phase behavior of a colloidal suspension under confinement is expected to be dramatically different from a bulk system. A series of experiments by Grier and co-workers [2] brings out even greater surprise than this simple expectation. In a recent experiment [3], they confine a charge-stabilized colloidal suspension within a pair of charged glass plates and drive the colloidal spheres towards the charged walls by electrophoresis. Under this metastable condition they observe a crossover from a purely repulsive screened Coulomb interaction, more popularly known as the Derjaguin-Landau-Verwey-Overbeek potential [4] between a pair of colloidal spheres to an attractive interaction, fairly long-ranged parallel to the plates, over a region sufficiently close to the glass plates, where the colloidal particles form crystalline layers.

This intriguing observation leads us to analyze more carefully the consequence of the confinement effects, albeit in terms of known theoretical models. It is useful to recapitulate the conventional picture due to Debye and Hückel that describes the pair interaction between colloidal spheres in the bulk. The colloidal suspension can be thought of as an assembly of large spherical ions (macroions) surrounded by tiny counterions, released by the macroions for overall

charge neutrality, and additional impurity ions, all dispersed in a solvent (typically water). For simplicity we ignore the impurity ions. The tiny counterions screen the mutual Coulomb interaction between the macroions. According to the linear Debye-Hückel picture [5], in the absence of the macroions, the tiny counterions with mutual Coulombic interaction will be homogeneously distributed in space. Now suppose that two macroions are introduced at a certain separation. The presence of the macroions will disturb the distribution of the counterions. If the disturbance of the counterion density from the homogeneous situation is not too large, one can write the mean-field free-energy cost of such density inhomogeneity as a quadratic functional of the density difference and calculate the equilibrium density distribution of the counterions by minimizing the resulting free energy. If this counterion density distribution is integrated out of the free energy, one is left with an effective screened Coulomb repulsion between the macroions at a separation r : $v(r) = \exp(-\kappa r)/r$, where κ is inverse Debye screening length, given by $\kappa^2 = (4\pi e^2/\epsilon k_B T)q^2\rho$, e being the fundamental charge, $q(=1)$ the charge on the counterions, ϵ the dielectric constant of the solvent, and ρ the mean counterion density. Note that $1/\kappa$ is the length scale that determines the range of the repulsion. What do we expect if such a colloidal suspension is confined between two charged plates? Due to the electrostatic interaction of the walls, the distribution of the counterions released by the walls themselves will not be homogeneous even without the macroions, the density of the counterions being larger close to the walls. The inhomogeneous counterion density profile will generate an electrostatic external potential on the macroions. Furthermore, if one assumes that two macroions are introduced, not too close to the plates, and this disturbs the counterion density profile only slightly so that the linear Debye-Hückel picture would remain valid, one will still get a repulsive screened Coulomb interaction between the macroions, but now the inverse Debye screening length, being dependent on the counterion density, will be a function of the positions of the macroions with respect to the walls by virtue of the inhomogeneity of the counterion density profile. At low density of the macroions, the particles will tend to inhabit the center where the

*Also at Institute für Festkörperforschung, Forschungszentrum, Jülich, D-52425 Jülich, Germany.

external potential is minimum. However, with increasing density the central layer will be unstable to the formation of side layers. The side layers will be subject to the outward repulsion of the central layer and the inward repulsion due to the external potential. The balance between these two opposite forces would play a crucial role in the phase behavior as well as in the realization of the effect of the space-dependent screening in such systems.

We have carried out detailed Monte Carlo simulations to bring out the salient features of this competition that provide useful insight into the role of confinement on the colloidal suspensions. We observe that the system undergoes a sequence of different number of layers with increasing density of the macroions. The wall repulsion, however, tends to reduce the effect of the space-dependent screening, resulting in the fact that the phase behavior can be accounted for by a space-independent screened Coulomb interaction but with an effective inverse Debye screening length. Most significantly, we find that the side layers do not show up any crystalline order, the so-called *precrystallization* effect [6]. We account for the inhibition to precrystallization observed in our system through simple mean-field calculations.

Details of the derivation of the space-dependent screening have been given by Denton and one of us [7]. We give here only the relevant features of their derivation for the sake of clarity. The Poisson-Boltzmann equation for the counterions without the macroions for a situation of two infinitely charged walls at $z = \pm H/2$ can be solved exactly to yield the counterion density profile

$$\rho_w(z) = \frac{\epsilon k_B T}{4 \pi e^2} \frac{2 \pi^2}{H^2} \sec^2 \frac{\pi z}{H}.$$

The corresponding electrostatic potential can be shown to be $\phi(z)/k_B T = -(2/e) \ln(\cos \pi z/H)$, which acts as an external potential on the macroions. The interaction potential between a pair of macroions, assuming a small density perturbation induced by the macroions over $\rho_w(z)$, is given by

$$V(|\vec{r}_{||} - \vec{r}'_{||}|, z, z') = \frac{Q^2 e^2}{\epsilon} \frac{1}{r} \exp[-\kappa(z, z')r],$$

where Q is the surface charge on the macroion, $r = [(\vec{r}_{||} - \vec{r}'_{||})^2 + (z - z')^2]^{1/2}$ is the separation between two macroions, $\vec{r}_{||}$ and $\vec{r}'_{||}$ being their planar coordinates, and

$$\kappa^2(z, z') = \frac{4 \pi e^2}{\epsilon k_B T} \left[\frac{1}{z - z'} \int_z^{z'} dz_1 \rho_w(z_1) \right] + \kappa_0^2$$

is the square of the z -dependent inverse Debye screening length. Here κ_0 is the contribution to the screening from the counterions released by the macroions of density ρ_M : $\kappa_0^2 = (4 \pi e^2 Q / \epsilon k_B T) \rho_M$.

MONTE CARLO SIMULATIONS

The Monte Carlo simulations are performed on $N=192$ macroions in a parallelepiped geometry having periodic boundary condition (PBCs) in the x and y directions with the ratio of the dimensions L_x/L_y being $\sqrt{3}/2$ and no PBCs in

the z direction, where the particles, mutually interacting via the space-dependent screened potential, are subject to the external potential $\phi(z)/k_B T$. The starting configuration in each case has been three equally populated layers of a triangular lattice with slight random perturbations at each lattice site, one layer being at the center and the other two at $z = \pm H/4$. The particle positions are updated by a standard Metropolis algorithm. The first 10 000 Monte Carlo (MC) steps (each step being N attempts to move the particles) are discarded for equilibration, which is checked by monitoring the energy of the system. The next 10 000 steps are performed to calculate the different quantities of interest.

We report the results from our simulations for the system parameters $Q=1000$, particle diameter $d=10^{-4}$ cm s [8], $\epsilon=80$, and $T=300$ K, which are realistic for a colloidal suspension. For a given H we vary $\kappa^* = \kappa_0 H$, which is evidently equivalent to tuning ρ_M . We illustrate in detail the case of $H/d=20$. Figure 1(a) shows the density profile of the macroions $\rho(z)$ calculated by binning the z coordinates of the particles for different κ^* . $\rho(z)$ shows pronounced peaked structures, indicating the formation of layers. For very low κ^* , there is only one central layer. As κ^* increases, two symmetric side layers are formed and the central one decays considerably, resulting in a two-layer situation. Increasing κ^* further, we get a cascade of the formation of several layers. The position vectors of the particles lying within the half-width of a peak are projected onto the constant $z = z_m$ plane, where z_m is the position of the peak, and this projected plane is identified as a layer located at $z = z_m$. For such a layer, we calculate the bond orientation order parameter defined by

$$\psi_6 = \left\langle \frac{1}{N} \sum_{\alpha=1, N} \frac{1}{6} \sum_{\beta} \exp(i6\Theta_{\alpha, \beta}) \right\rangle,$$

where the angular brackets indicate the configuration average and $\Theta_{\alpha, \beta}$ is the angle between a fixed axis (here the x axis) and the bond joining a particle α with another particle β lying within a radius $1/[\rho(z_m)]^{1/2}$ around α , $\rho(z_m)$ being the area density at the peak. The quantity $|\psi_6|^2$ is clearly sensitive to local crystalline order in the layer: $|\psi_6|^2 = 0$ for a fluid (L) phase and $|\psi_6|^2 \neq 0$ for a crystal (S) phase of hexagonal order. We find that the layers found under different situations have fluid order (L). The sequence of transition for $H/d=20$ is clearly $nL \rightarrow (n+1)L$ type. We get an identical sequence for $H/d=40$ as well.

We show in Fig. 1(b) the space-dependent inverse Debye screening length $\kappa(0, z)H$ as a function of z for $\kappa^*=4.4$ where the system shows $2L$ arrangement. Clearly, the inverse Debye screening length does not change appreciably from $\kappa^2(0, 0) = 2 \pi^2/H^2 + \kappa_0^2$ over the position of the side layers. We repeat our simulations for the same κ^* by setting $\kappa(z, z') = \kappa(0, 0)$ but under the identical external potential and get a density profile insignificantly different from the space-dependent case, as is apparent in Fig. 1(a). We thus conclude that the system behaves to a large extent as if with an effective inverse screening length $\kappa_{eff} = \kappa(0, 0)$, independent of z . Note that $\kappa_{eff}^2 > \kappa_0^2$, an enhancement of the screening proportional to $1/H^2$, completely due to the confinement induced by the charged plates.

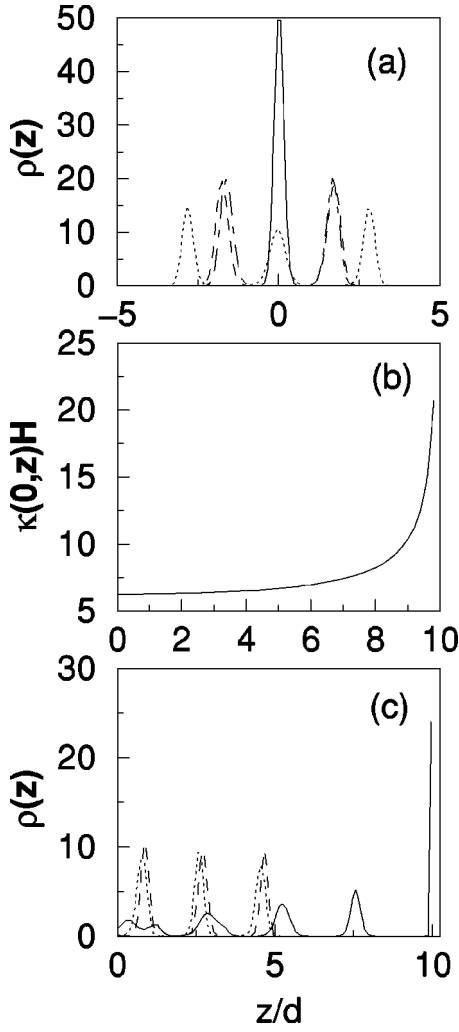


FIG. 1. (a) Density profile $\rho(z)$ vs z plot from simulations for $\kappa^*=0.5$ (solid line), $\kappa^*=4.4$ (dashed line), and $\kappa^*=6.0$ (dotted line) with the space-dependent screening and $\kappa^*=4.4$ with the space-independent screening (dot-dashed line). The space-dependent and the space-independent cases are almost indistinguishable. (b) $\kappa(0,z)H$ vs z plot for $\kappa^*=4.4$. (c) $\rho(z)$ vs z plot with $\kappa^*=15.0$ for the hard-wall case (solid line), the space-independent screening (dashed line), and the space-dependent screening (dotted line). $H/d=20$ in all the cases.

To identify the generic effect of the confinement due to the charged plates, we compare our results ($\kappa^*=15.0$) with a situation of screened Coulomb particles with inverse screening length κ_{eff} , confined by two hard walls, namely, in an external potential $V_0\delta(z\pm H/2)$ with $V_0=\infty$ instead of $\phi(z)/k_B T$. The density profile, shown in Fig. 1(c), indicates an extremely sharp and strong layer close to the hard walls, in contrast to relatively broader and weaker side layers formed in the presence of the external potential for both the space-dependent and the space-independent screenings. An immense qualitative difference is immediately apparent from the snapshots in Fig. 2. The snapshots of three configurations (5000 MC steps apart after equilibration) in the layer close to the hard walls, shown in Fig. 2(a), clearly indicate an onset of precrystallization [6], which is further supported by a high value of $|\psi_6|^2$ ($=0.44$). To the contrary, the precrystallization is completely absent in the other cases, as is apparent

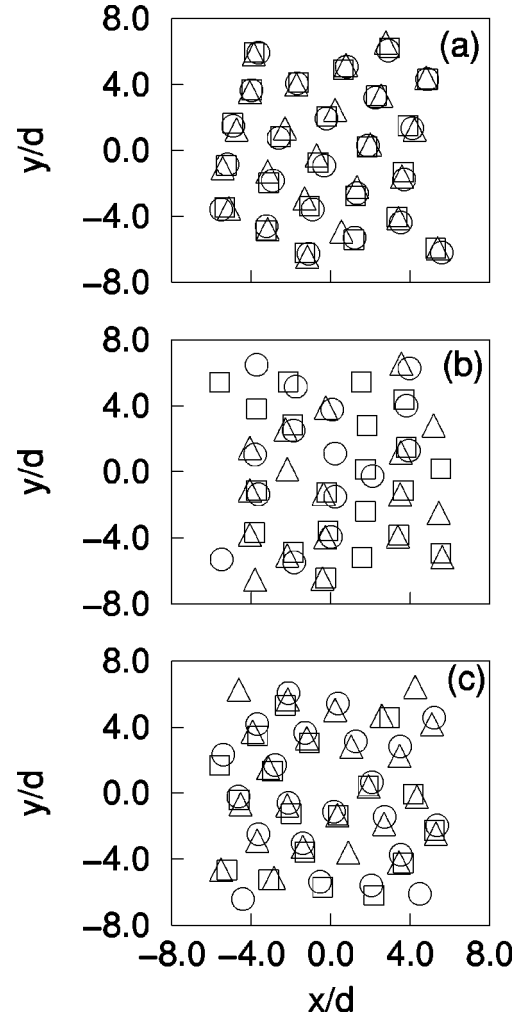


FIG. 2. Snapshots of the outermost layer [Fig. 1(c)] for three well-equilibrated configurations, 5000 MC steps apart (circles, step 0; squares, step 5000; triangles, step 10 000 after equilibration), with $\kappa^*=15.0$ and $H/d=20$. (a) The hard-wall case, (b) the space-independent screening, and (c) the space-dependent screening in the presence of the external potential. The onset of precrystallization in (a) and its absence in (b) and (c) are noteworthy.

from the snapshots depicted in Figs. 2(b) and 2(c). We have explicitly verified that our results do not change under longer runs for the same system size and for a larger system size ($N=768$).

MEAN-FIELD THEORY

The inhibition to the precrystallization can be understood by considering the mean-field energetic coupling $\frac{1}{2}\int V(r_{||},z,r'_{||},z')\rho(r_{||},z)\rho(r'_{||},z')$ between the layers. For simplicity we treat the system with three layers and ignore the in-layer structure and their widths. In this tremendously simplified picture, $\rho(r_{||},z)=\rho_s\delta(z-z_0)+\rho_c\delta(z)+\rho_s\delta(z+z_0)$, where ρ_c is the area density at the central layer and ρ_s is the area density of the two side layers situated at $z=\pm z_0$, satisfying the constraint $2\rho_s+\rho_c=\rho_M H$. The resulting mean-field energy per unit area, including the external potential contribution, can be written as $E=A(z_0)\rho_s^2+B(z_0)\rho_s$, where

$$A(z_0) = \frac{2\pi e^2}{\epsilon} Q^2 \left[\frac{1}{\kappa_s} + \frac{2}{\kappa_c} - 4 \frac{\exp-(z_0 \kappa_d)}{\kappa_d} + \frac{1}{2} \frac{\exp-(2z_0 \kappa_d)}{\kappa_d} \right],$$

$$B(z_0) = \frac{2\pi e^2}{\epsilon} Q^2 \left[\frac{\epsilon k_B T}{4\pi^2 e^2} \frac{(\kappa_0 H)^2}{QH} \left(\frac{\exp-(z_0 \kappa_d)}{\kappa_d} - \frac{1}{\kappa_c} \right) \right] + 2Q\phi(z),$$

$\kappa_c = \kappa(z=0, z'=0)$, $\kappa_s = \kappa(z=z_0, z'=z_0)$, and $\kappa_d = \kappa(z=0, z'=z_0)$. Note that a one-layer structure is given by $\rho_s = 0$. The transition to the three-layer structure, with $\rho_s \neq 0$, will involve the change in sign of $A(z_0)$ in the (k^*, z_0) plane for a given set of system parameters $(Q, H/d, \epsilon k_B T)$. Once, however, the three-layer structure emerges, the outward migration of the side layers, involving no further change of sign of $A(z_0)$, will be governed by the competition between different terms of $B(z_0)$. The z_0 dependence of $B(z_0)$ comes from the repulsion on the side layers by the central layer that pushes the side layers outward, given by

$$\frac{2\pi e^2}{\epsilon} Q^2 \left[\frac{\epsilon k_B T}{4\pi^2 e^2} \frac{(\kappa_0 H)^2}{QH} \right] \frac{\exp-(z_0 \kappa_d)}{\kappa_d},$$

and the external potential that pushes them inward. With increasing κ^* , the repulsion due to the central layer increases, pushing the side layers closer to the walls, but the external potential repels them strongly, preventing their outward movement, as well as restricting their populations, which in turn would disfavor the possibility of the in-layer symmetry breaking, namely, from liquid order to crystal order. Note that the essence of the argument does not change, even if the screening does not depend on z .

To make this qualitative picture more apparent, we minimize the free energy per unit area $F = 2\rho_s \ln \rho_s + \rho_c \ln \rho_c + E$ and the area densities ρ_s and ρ_c at the minimum are mapped to an effective two-dimensional hard-disk system through the Barker-Henderson (BH) perturbation theory [9] to identify the phases in different layers. So far the effective hard-disk area fraction does not exceed the random close-packed limit ($=0.9$); we identify a layer to have crystal order (*S*) if it exceeds 0.7, otherwise the order is taken to be fluid (*L*) [10]. The numerical calculations are performed for the same parameters as in the simulations. We find a sequence of ordering (Fig. 3) $1L \rightarrow 1S \rightarrow LLL \rightarrow LSL$ with increasing κ^* , where the middle letter indicates the phase at the central layer and the outer ones those in the side layers [11]. This sequence clearly indicates a situation opposite to precrystallization, which qualitatively supports our simulation observations. However, we do not find *LSL* ordering in our simulations. The simulations show that beyond $3L$ order the system becomes unstable to the formation of more than three layers, which is obviously not accounted for in our theory. The presence of the *1S* layer in our theory rather than the *2L* layers found in the simulations is presumably an artifact due to neglecting the width of the layers.

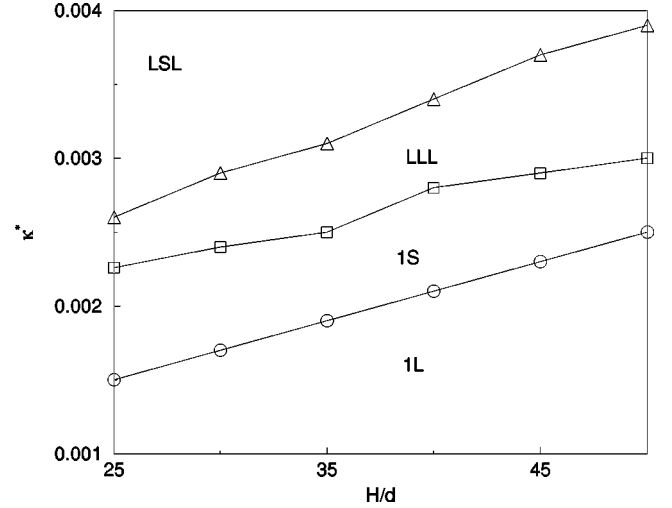


FIG. 3. Mean-field phase diagram in the H/d - κ^* plane. The solid lines are guides to the eye.

CONCLUSION

We conclude the paper by stressing the fact that a colloidal suspension confined in a pair of charged plates is characterized by the marked absence of the *precristallization* tendency. Careful experiments will be needed to verify this interesting consequence of the confinement. Since we ignore the impurity ions here, we expect our prediction to hold in the cases of strongly deionized colloids. Our analysis ignores the effect due to the image charges, which amounts to assuming that there is no discontinuity of the dielectric constant across the plates, which is present though across the charged glass plates in the experiment [3]. However, the image charges do not produce essentially different effects in the linear theory [12]. More importantly, however, the nonlinearities due to the bilayers formed in the vicinity of the charged walls, neglected in our work, coupled with the effect of the image charges, lead to the experimentally observed crossover from interparticle repulsion to attraction, as has been shown very recently [13]. This crossover takes place over a region sufficiently close to the walls, typically not explored by the particles in the system in our work, which gives *a posteriori* justification to the linear theory in the regime that we have considered here. Nevertheless, it will be worth carrying out first-principles simulations in the direction of Ref. [14] for confined colloids to verify the important nonlinear effects along with that due to the image charges. More theoretical calculations on our model, especially the inclusion of the width of the layers and the in-layer order parameters rather than the BH mapping, would certainly be important. We hope to report some of these studies in the future.

ACKNOWLEDGMENTS

We thank Daan Frenkel, Matthias Schmidt, and Anne Denton for helpful discussions. J.C. thanks OSPT for financial support and DFG (Grant No. SFB 237) for its hospitality during which a part of the work was done.

- [1] A. K. Sood, in *Solid State Physics*, edited by E. Ehrenreich and D. Turnbull (Academic, New York, 1991), Vol. 45; H. Löwen, *Phys. Rep.* **237**, 249 (1994); J. Chakrabarti, S. Sengupta, H. R. Krishnamurthy, and A. K. Sood, in *Ordering and Phase Transitions in Charged Colloids*, edited by A. K. Arora and B. V. R. Tata (VCH, New York, 1996).
- [2] J. G. Crocker and D. G. Grier, *Phys. Rev. Lett.* **73**, 352 (1994); *J. Colloid Interface Sci.* **179**, 298 (1996); *Phys. Rev. Lett.* **77**, 1897 (1996); A. E. Larsen and D. G. Grier, *ibid.* **76**, 3862 (1996).
- [3] A. E. Larsen and D. G. Grier, *Nature (London)* **385**, 230 (1997).
- [4] B. V. Derjaguin and L. Landau, *Acta Phys. (USSR)* **14**, 633 (1941); E. J. W. Verwey and J. Th. G. Overbeek, *Theory of the Stability of Lyophilic Colloids* (Elsevier, Amsterdam, 1948).
- [5] H. Löwen, P. A. Madden, and J. P. Hansen, *J. Chem. Phys.* **98**, 3275 (1993).
- [6] D. J. Courtemanche, T. A. Pasmore, and F. Van Swol, *Mol. Phys.* **80**, 861 (1993); T. Biben, R. Ohnesorge, and H. Löwen, *Europhys. Lett.* **28**, 665 (1994); M. Schmidt and H. Löwen, *Phys. Rev. E* **55**, 7228 (1997).
- [7] Anne M. Denton and H. Löwen, *Thin Solid Films* (to be published).
- [8] However, we do not account for the hard-core (particle) diameter in our calculations.
- [9] J. P. Hansen and I. R. McDonald, *Theory of Simple Liquids* (Academic, New York, 1986).
- [10] H. Weber, D. Marx, and K. Binder, *Phys. Rev. B* **51**, 14 636 (1995).
- [11] With the space-independent screening, however, we find only $1L \rightarrow 1S$ in a comparable regime.
- [12] D. Goulding and J. P. Hansen, *Mol. Phys.* (to be published).
- [13] D. Goulding and J. P. Hansen (unpublished).
- [14] I. D'Amico and H. Löwen, *Physica A* **237**, 25 (1997); H. Löwen and G. Kramposthuber, *Europhys. Lett.* **23**, 673 (1993). Interestingly, even without the image charges, such calculations predict the presence of short-range attraction; see E. Allahyarov, I. D'Amico, and H. Löwen, *Phys. Rev. Lett.* (to be published).